Geophysical Research Letters

RESEARCH LETTER
10.1002/2018GL077244

Key Points:
- Global cross correlation of earthquake coda reveals the Earth's correlation wavefield that consists of numerous correlated phases
- The similarity between the observed and synthesized correlation wavefields indicates that the Earth's radial structure is well constrained
- Correlated phases are explained by interference of a pair of seismic phases with the same ray parameter and a subset of legs in common

Supporting Information:
- Supporting Information S1

Correspondence to:
T.-S. Phạm,
thanhson.pham@anu.edu.au

Citation:
Phạm, T.-S., Tkalčić, H., Sambridge, M., & Kennett, B. L. N. (2018). Earth's correlation wavefield: Late coda correlation. *Geophysical Research Letters*, *45*, 3035–3042. https://doi.org/10.1002/2018GL077244

Received 24 JAN 2018
Accepted 18 MAR 2018
Accepted article online 26 MAR 2018
Published online 13 APR 2018

Earth's Correlation Wavefield: Late Coda Correlation

Thanh-Son Phạm[1], Hrvoje Tkalčić[1], Malcolm Sambridge[1], and Brian L. N. Kennett[1]

[1]Research School of Earth Sciences, Australian National University, Canberra, ACT, Australia

Abstract Cross correlation of seismograms provides new information on the Earth both through the exploitation of ambient noise and specific components of earthquake records. Here we cross-correlate recordings of large earthquakes on a planetary scale and identify a range of hitherto unobserved seismic phases in Earth's correlation wavefield. We show that both arrivals with the timing expected for the regular seismic wavefield and previously unexplained phases are produced by interference between seismic paths having the same ray parameter but with only a subset of propagation legs in common. This insight explains the origin and generation mechanism of the features of Earth's correlation wavefield and opens up new ways of addressing issues in global seismology. Strong similarity between observed and synthesized correlation wavefields indicates that the Earth's radial structure is remarkably well constrained in the intermediate period range.

Plain Language Summary We investigate the nature of earthquake coda waveform cross correlations and provide an explanation for the origin of, what we term here, the Earth's correlation wavefield. This consists of numerous correlated signals some that appear similar to regular seismic phases and others not apparent in the conventional seismic wavefield. The nature of the correlation wavefield described here has far-reaching implications for the field of seismology. In particular, we show that the correlated wavefield illuminates the Earth's interior in an entirely new and unexpected manner. With further method developments we expect this to lead to improved structural constraints on the Earth interior, especially in the poorly sampled regions such as the Earth's lowermost mantle and core.

1. Introduction

The discovery and exploitation of long distance-range correlation in the ambient seismic wavefield (Campillo & Paul, 2003; Shapiro et al., 2005) has created new forms of subsurface tomographic imaging. Previously, noisy data sets had simply been discarded in earthquake seismology. However, by stacking multiple cross-correlation functions of ambient noise or seismic coda recorded on a pair of recorders, an approximation to the elastic response of the Earth between these two recorders (Green's functions or Earth structure kernels) can be routinely retrieved. Because this approach is nearly independent of precise earthquake source parameters, the impact of all uncertainties associated with the seismic source can be avoided. Early studies focused on extracting surface wave dispersion and its use in tomographic inversion for structure at depth (e.g., Bensen et al., 2007; Lin et al., 2007). Later studies showed it was possible to retrieve signals of body waves sensitive to the seismic discontinuities in the Earth's lithosphere (Poli et al., 2012; Zhan et al., 2010).

More recent studies applying cross correlation to the late coda of seismic records of major earthquakes (Lin et al., 2013; Lin & Tsai, 2013; Sens-Schönfelder et al., 2015) have observed signals sensitive to the Earth's deepest interior, in the core (Boué et al., 2013; Nishida, 2013). The properties of such phases, particularly travel times, have been used to infer physical properties of the deep Earth (e.g., Huang et al., 2015; Wang et al., 2015). A range of terms have been coined to describe these new methods including *global interferometry* and *global cross correlation*. Application of such approaches to the ever-growing volume of digital seismic data is likely to significantly advance studies of the Earth's deep interior, especially for the poorly sampled inner core (Tkalčić, 2017).

In these global coda cross-correlation studies, some apparent phases have the character of seismic body waves (e.g., ScS, PKIKP, and PcPPKP waves). However, Boué et al. (2014) showed that main signals seen in earthquake-related cross correlogram have anomalous amplitudes and contain unexplained arrivals. More recently, it has been found that the coda wavefield does not have the energy equipartition property that is a prerequisite for accurate retrieval of the Green's function (Sens-Schönfelder et al., 2015). Poli et al. (2017) have proposed a normal mode framework to explain the existence of the arrivals similar to ScS (on the

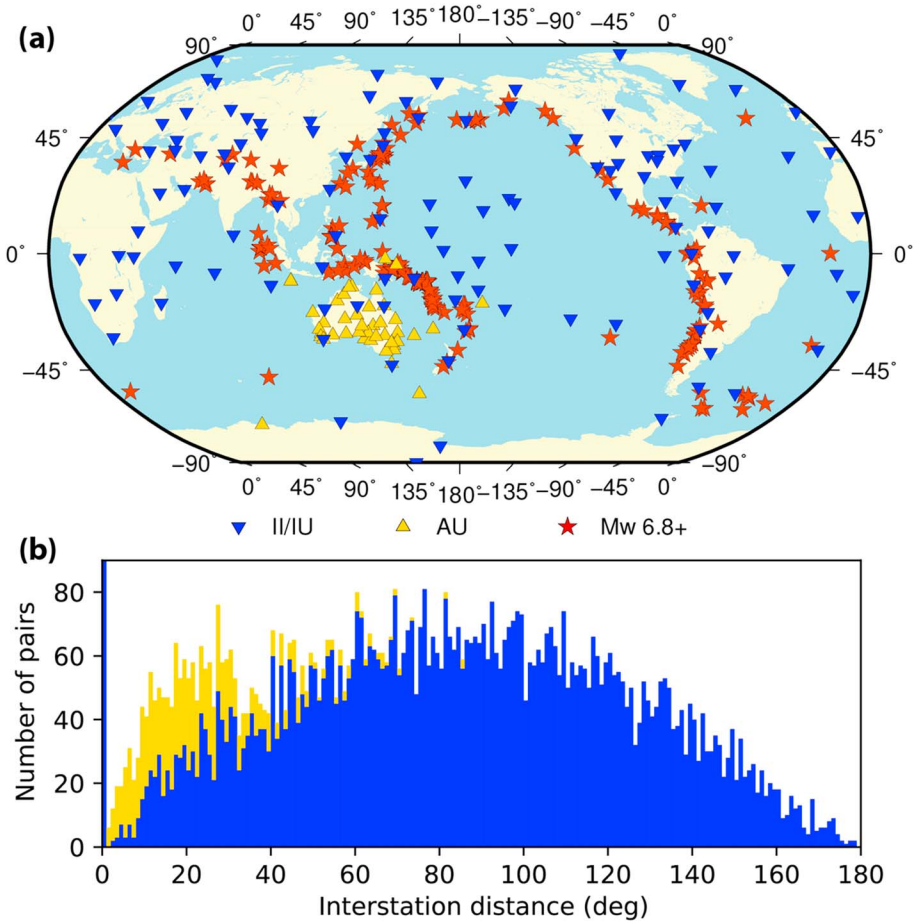

Figure 1. (a) Map of stations and earthquakes used in this study. Stations originate from three networks, the Australian National Seismograph Network (network code AU), the Global Seismographic Networks administrated through Incorporated Research Institutions for Seismology (network code IU and II). Mw6.8+ earthquakes from the time interval 2010–2016, cataloged in the global centroid moment tensor catalogue, are marked by red stars. (b) Istogram of interstation distances with 1° bin size. The frequency histogram of interstation distances of the combined IU and II global networks is in blue, and the frequency histogram determined from the AU network is in yellow.

vertical component in stacked coda autocorrelations). We note that there are many other prominent signals from the late coda cross correlations that are not the standard seismic phases recognized in the seismic wavefield (as can be seen in Figures 2 and S1 in the supporting information). Our work demonstrates that these additional phases cannot be interpreted to be part of the surface focus Green's function in a comparable way to the surface waves obtained from ambient noise (Shapiro et al., 2005; Shapiro & Campillo, 2004). The interpretation of correlation results as resulting from a surface focus source (e.g., Huang et al., 2015; Wang et al., 2015; Xia et al., 2016) is thus incomplete.

Here we provide an alternate explanation of the complete range of body wave phase arrivals seen in the correlation wavefield that does not invoke an interpretation in terms of a Green's function. Rather, we argue that all the observed correlation wavefield arrivals for the late coda are produced by interferences between phases with the same ray parameter but with only a subset of propagation legs in common.

2. Global Waveform Coda Cross Correlogram

We use digital waveform data from the Global Seismographic Network (marked by triangles in Figure 1a) to construct global cross correlograms of all available waveform pairs (Figure 1b) in the intermediate period band 15–50 s. The data processing employs the temporal normalization (Lin et al., 2007) to suppress dominating contribution of high-amplitude surface waves or aftershocks, then the spectral whitening normalization (Phạm & Tkalčić, 2017) to balance contribution of all frequencies (see Methods section in the supporting

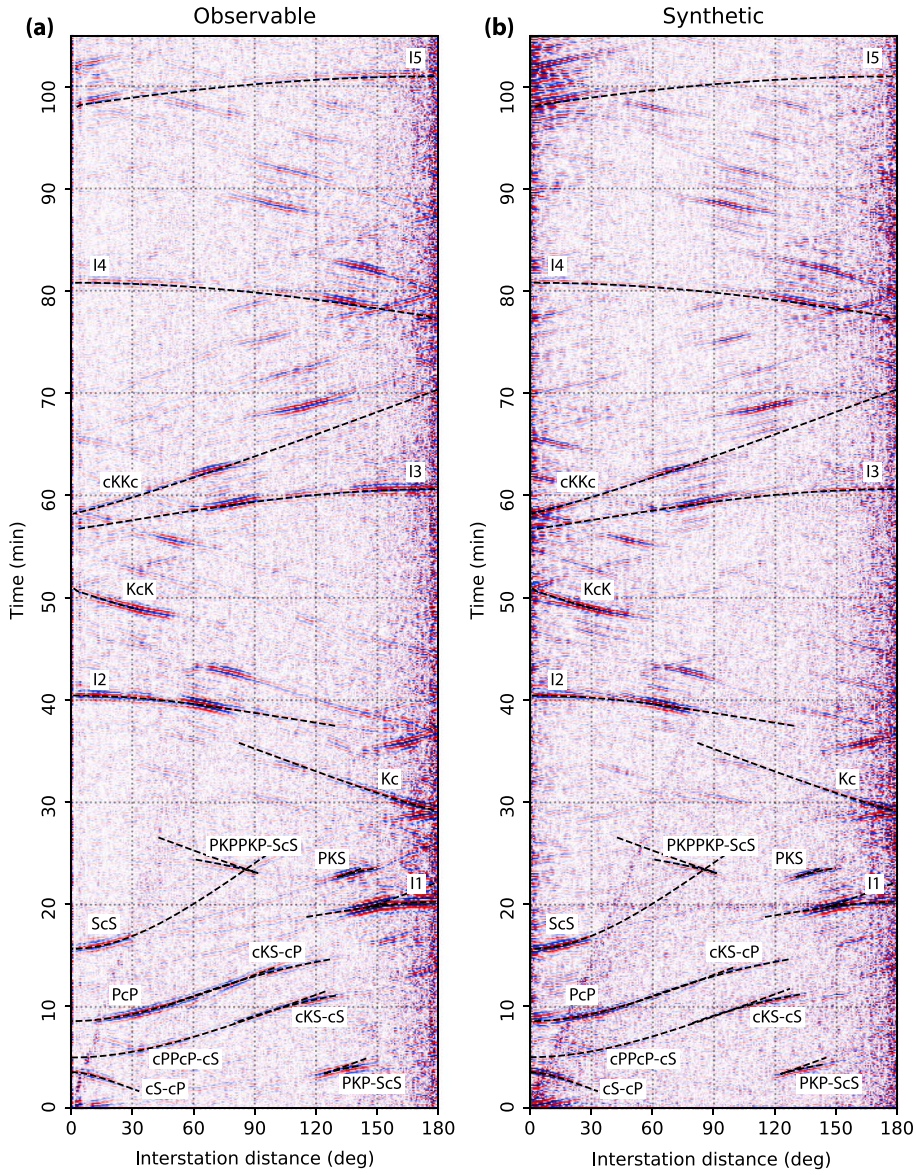

Figure 2. The Earth's correlation wavefield. (a) Observed and (b) synthetic cross correlograms for the binned interstation distance with bin size of 1° (see Methods section in the supporting information). Cross correlograms are prefiltered in the period band of 15–50 s. Red and blue colors show the positive and negative amplitudes. Dashed travel time curves with corresponding phase names are predicted using the reference model ak135 (Kennett et al., 1995) (see the main text for the explanation of the naming convention). See Methods sections in the supporting information for the derivation of travel time curves of noncausal phases.

information). We exploit vertical component seismograms of earthquakes with Mw $\geq$ 6.8 according to the global centroid moment tensor catalog (Ekström et al., 2012) and extract the coda waveforms for the time interval 10,000–35,000 s (~3–10 hr) after the origin time. The time window and the magnitude threshold we have employed are those recommended in previous studies that analyzed the emergence of few individual correlation phases that are sensitive to the core (e.g., Lin & Tsai, 2013; Wang et al., 2015; Xia et al., 2016). We find that this window does indeed produce results of high quality. The stack of the cross-correlogram results can be thought of as a realization of part of the Earth's *correlation wavefield*. Figure 2a shows the observed cross-correlogram field as a function of the angular distance between stations and the correlation lapse time, which contains pronounced correlated peaks with lapse times of up to 2 hr. At first glance, a number of correlated features appear to represent conventional seismic phases. In an interferometric framework, these phases would be explained as the Earth's response after a signal has been initiated by a virtual source

collocated with one station and recorded on the other station of each pair. Indeed, the delay times of many of the correlated peaks match well with theoretical travel time curves for a source at the Earth's surface (Kennett et al., 1995). The most obvious observed seismic phases in the early time part of the cross correlograms (Figure 2) are proxies for PcP and PKP waves and their combinations. At later times in the cross-correlogram field, the dominant features are proxies for PKIKP multiples representing up to five passages through the Earth's inner core. Such phases have not previously been observed in the earthquake wavefield, and their complicated raypaths render the standard phase name convention used in seismology rather cumbersome. Here we adopt a simplified convention in which only the central part of the standard phase's standard name is retained, to indicate the deepest Earth layer traversed by the raypath. With this convention, PcP is abbreviated as c, PKPPcP is abbreviated as Kc, PKIKP is abbreviated as I, and PKIKPPKIKPPKIKP becomes I3. Among other prominently observed phases in the correlation field with large lapse times (Figure 2) are Kc, KcK, cKKc, I2, I3, I4, and I5. To our knowledge, several of these phases have never previously been identified in any earthquake record nor in cross-correlation studies (e.g., cKKc, I3, I4, and I5).

We also observe several prominent phases that appear to be noncausal in nature in that they precede the direct *P* arrivals and thus have no counterparts in the conventional seismic wavefield. For example, five such phases, marked in Figure S1, are clearly seen arriving ahead of the *P* waves. One of them, which we refer to below as cS-cP, was previously noted but not further analyzed nor explained by Boué et al. (2014). It is worth noting that these additional arrivals appear in the stack of continuous seismograms for days containing big earthquakes (see Boué et al., 2014, Figure 4b), while they are absent in the stack of the seismically quiet days. This suggests that the origin of the noncausal arrivals must be closely related to the nature of the seismic wavefield in the later parts of the coda. We argue that any complete understanding of the observed correlation wavefield must by necessity also explain these phases.

In Figure 2b we compare the Earth's observed correlation wavefield to a synthetically generated one. We use a numerical simulation in a spherical Earth to generate synthetic coda waveforms based on the actual configuration of earthquakes and seismic recorders. We use the axisymmetric spectral element method, AxiSEM (Nissen-Meyer et al., 2014), with a dominant period of 10 s. The velocity and density meshes are taken from the ak135 reference model (Kennett et al., 1995) with the elastic attenuation model of Montagner and Kennett (1996). Explosive sources and seismic stations are located at their actual geographic coordinates (as in Figure 1). Ten-hour-long vertical-component synthetic seismograms were calculated to include the coda window used in this study (see Methods in the supporting information). These synthetic data were processed in an identical way to the observed data.

The similarity between the observed and synthetic cross correlograms is strong, which we consider quite remarkable. It is clear that almost all features detected in the observed cross correlogram can be identified in the synthetic cross correlogram and vice versa. This similarity confirms that in the 15–50-s period range all the observed features are predominantly a result of interactions of seismic waves with the Earth's radial structure and not due to scattering from Earth's lateral heterogeneities (Sens-Schönfelder et al., 2015) since we use just a radial (1-D) model.

3. Explanation of Phase cS-cP

The cS-cP phase is a prominent signal in the Earth's correlation wavefield (Figures 2 and S1). This phase arrives in the 3–4-min range of lapse time with a negative moveout. The delay time diminishes with increase of interstation distance, behavior that is not observed for regular seismic phases. The cS-cP phase has remained mysterious since the first observation (Boué et al., 2014) and is mentioned in passing in a recent study that focused on the explanation of ScS arrivals at near-vertical incidence (Poli et al., 2017).

We now show how such a novel phase can arise in the process of waveform correlation and thereby provide the basis for explaining the full range of other anomalous arrivals in both the observed and synthetic cross correlograms (see Figure S1 for four other phases).

The origin of the phase cS-cP is closely linked to the core-mantle boundary (CMB), a major internal discontinuity within the Earth with a pronounced seismic contrast between the solid mantle and the liquid outer core comparable to that of the Earth's free surface. When a seismic wavefront reaches the CMB, any point on the CMB can be thought of as a secondary source (i.e., via Huygens' principle—see Figure 3a). Such a virtual

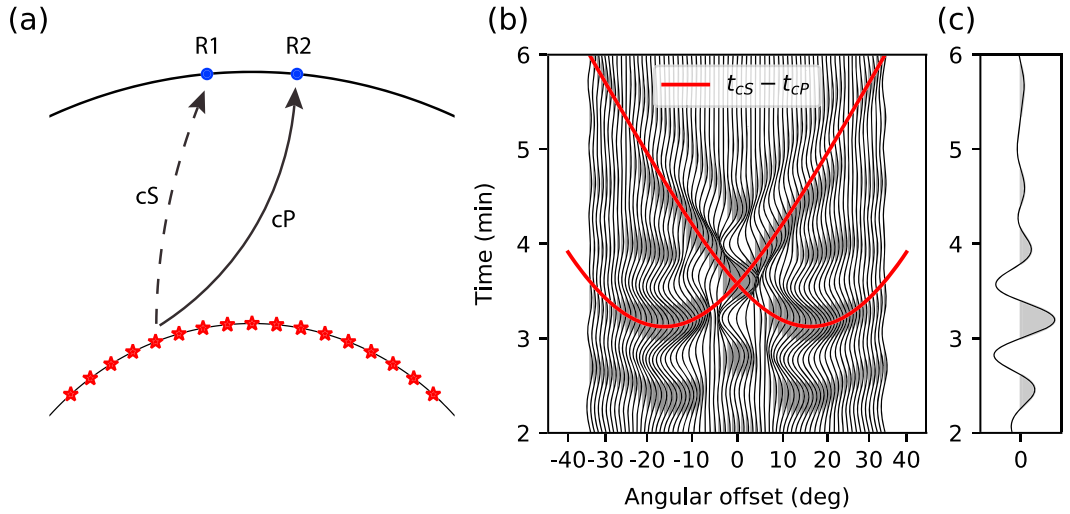

Figure 3. Explanation based on the stationary point principle for the correlated phase cS-cP. (a) Hypothetical Huygens' sources on the core-mantle boundary (CMB) radiate seismic waves to receivers R1, R2 on the Earth's surface. (b) Red curves show differential travel time of cS and cP ($t_{cS} - t_{cP}$) as a function of angular offset between the CMB source and the midpoint of two receivers. The background shows synthetic correlation waveforms of two stations from an explosive source located at the corresponding CMB location. (c) Stacked cross-correlation waveform for all CMB sources demonstrates the emergence of a peak around the stationary point of the differential travel time curves.

source radiates *P* and *S* waves that travel along different geometrical raypaths to receivers on the Earth surface. A recorded seismogram can be thought of as a superposition of an infinite number of individual-source seismograms corresponding to those secondary sources. The resulting cross correlogram is a stack of individual-source cross correlations (Wapenaar et al., 2010).

Consider the cross correlation of *S* and *P* waves that are simultaneously radiated from a single CMB source through a 1-D Earth to be recorded by two receivers R1 and R2 located at an arbitrary interstation distance (Figure 3a). The differential travel time ($t_{cS} - t_{cP}$) varies as a function of the angular offset of the CMB source from the receiver R1. The nearly parabolic differential travel time curve (Figure 3b) has a saddle point at its minimum, with a symmetrically equivalent one on the other side of the midpoint of the receiver pair. When contributions from different CMB sources are stacked, constructive interference occurs around the saddle point, with destructive interference elsewhere. As a result, a strong correlated phase emerges in the resulting stacked cross correlations (Figure 3c). The resulting cross correlogram has a negative moveout, which corresponds directly to the observed and synthetic results (Figures 2a and 2b). We refer to this correlated phase as cS-cP, indicating the travel time difference of *P* and *S* arrivals from a common origin at the CMB "c."

The concept of constructive interference corresponding to the stationary phase principle (Snieder, 2004) has been widely used (e.g., Boschi & Weemstra, 2015; Wapenaar et al., 2010). We do not observe similar signals between two *P* and two *S* waves because their minimum differential time vanishes.

When the two stations coalesce, the cross correlation becomes the autocorrelation, and the stationary source at the CMB lies directly beneath the recorder. This situation provides a unique probe through the mantle for measuring the differential travel time of *P* and *S* waves in the radial direction. In general, the angular offset of the stationary point from R1 increases with the interstation distance (see Figure S2).

The existence of a stationary point location on the CMB as a function of the interstation distance between R1 and R2 is equivalent to the requirement that the *P* and *S* waves have the same ray parameter, *p*, a value that can be specified for a given interstation distance. We can provide an alternative description in terms of the compressional *P* wavefield, reaching the CMB with the incoming energy partitioned to *P* and vertically polarized shear waves. The partitioned energy of *P* and shear waves then yields two similar waveforms recorded at the stations R1 and R2. The similarity is manifested through the data processing and cross correlation as the phase cS-cP in the Earth's correlation wavefield. Figure 4a shows four levels of reverberation legs (i.e., reflection or transmission) of seismic rays from major discontinuities in the Earth's interior before reaching the

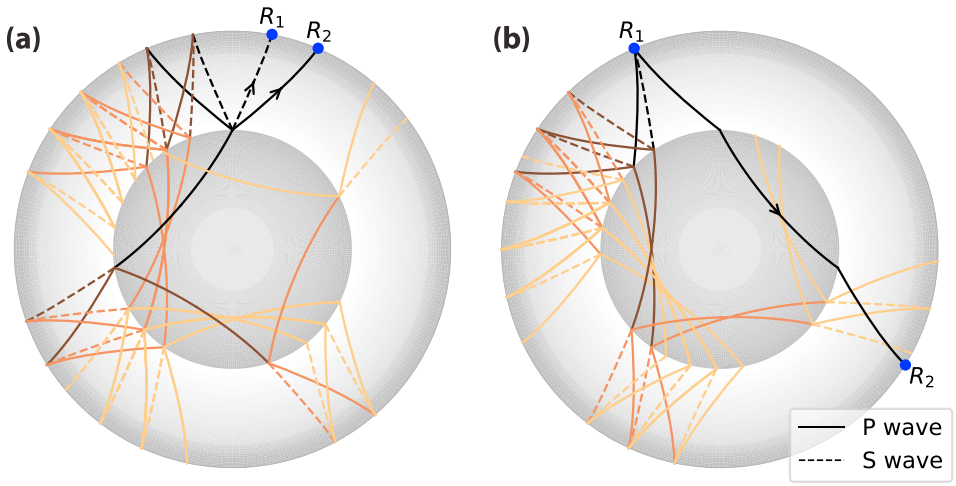

Figure 4. Geometrical raypaths contributing to two correlation phases: (a) cS-cP and (b) PKP. All legs including *P* and *S* legs from the mantle and K (*P* wave) leg from the outer core have the same ray parameter. *P* wave legs are shown with solid lines and *S* wave legs with dashed lines. The darker paths represent rays that contribute more directly to the correlation phases (see the text for more details).

stationary point. All these path combinations have the same ray parameter *p*. An earthquake that occurs near the intersections of these raypaths with the surface along the great circle can contribute to the formation of cS-cP, even though this contribution may be small. Each of the contributions to cS-cP comes from a single earthquake. We sum all contributions with a common station separation to produce the correlated phase and so build on many small contributions for pairs of regular phase combinations with all other legs in common. The number of possible combinations grows exponentially as a function of the number of reverberation levels, and thus, when correlations are made along an extended coda window, there are many possible ways of producing the phase pairs. Contributions from paths with high numbers of legs are more attenuated through reverberations within the Earth, and so it is reasonable to assume that the main contributions come from paths with a relatively small number of reverberative legs.

4. Earth's Correlation Wavefield

Guided by this explanation of the formation of the correlation phase cS-cP, we can explain other anomalous phases that emerge in Earth's correlation wavefield (see Figure S1). Consider cPPcP-cS, cKS-cP, cKS-cS, and PKP-ScS, whose stationary phase results are shown in Figure S3. In all cases, a stationary source for the differential travel times lies either on the CMB or on the Earth's surface. The stationary point of the differential travel time curves is maximal in these cases, rather than a minimum as for cS-cP. In all cases the raypaths from the stationary sources always arrive at the receivers with the same ray parameter. In consequence, there is a good fit of the predicted differential travel time curves to the anomalous phases in the observed and synthetic cross correlograms (Figures 2a, 2b, and S1).

If our assertion is correct that all observed arrivals are generated by interference between rays with common ray parameter and reverberation legs, then the question is "How then can the same physical mechanism be used to explain the observations of other arrivals that resemble the regular phases of the conventional seismic wavefield?" Here we consider the formation of the core phase PKP, but the arguments can be generalized for any conventional phase in the correlation wavefield. The way in which PKP stationary point is formed is shown in Figure S4. A correlation phase with the travel time properties of PKP can be formed from the interaction of two other phase pairs, namely, PcPPKP-PcP and PKPPcP-PcP. In general, the PcP part that is in common can be replaced by any other suite of raypaths (e.g., ScS, PKIKP, or PKiKP). Similar to the case of cS-cP phase, Figure 4b illustrates a number of possible raypaths that can contribute to the formation of the correlated phase PKP (excluding the contributions from the inner core for simplicity). Consequently, the phase with the timing of PKP that emerges on the cross correlograms in Figure 2 not only encapsulates the

information of the structure described by the geometric raypath corresponding to PKP waves but includes a multitude of phases that differ only in a leg corresponding to PKP.

In summary, the cross correlograms illustrated in Figure 2 are the observed and synthetized representations of the Earth's correlation wavefield. All phases seen in the correlation wavefield are the result of differences of pairs of seismic phases with amplitudes controlled by relative excitation in the coda field. The cross correlation and stacking of waveforms promotes differential phases that have the same ray parameter at the two stations (see Figure S5).

5. Discussions and Concluding Remarks

Ruigrok et al. (2008) undertook a theoretical study of the correlation of seismograms at the global scale. Their work with acoustic waves points out the way that correlation of a pair of seismic phases can isolate specific seismic phases, with an equivalence to virtual internal sources. Our results confirm their insight. A full theory for all the observable phases produced by correlation can be developed with a generalized ray representation of the late coda wavefield.

We present observations of the Earth's correlation wavefield using the coda of large earthquakes in the window of ~3–10 hr after their origin time, for the intermediate frequency band of 15–50 s. The results reveal a number of hitherto unobserved seismic phases such as high order inner core multiples I3–I5. The observations match well with comparable processing of synthetic waveforms based on a radially symmetric Earth model. The new phases should allow refinement of average Earth structure at depth. In this study we use the same late coda window and magnitude threshold as employed in earlier studies that analyzed the emergence of few correlation phases. With improved understanding of the correlation field we can now look to tune these parameters for future specific studies.

Since a correlation phase can be formed from the difference of any pair of regular seismic phases, the population of correlated phases is significantly larger than those in the regular seismic wavefield. Especially at large delay times, there are many correlated phases that have not yet been explicitly identified. The method of computing differential travel times with common ray parameter, which uses existing travel-time calculation tools (Buland & Chapman, 1983; Crotwell et al., 1999; Stein & Wysession, 2003) (see Figure S5 and Methods section in the supporting information), provides the key to phase identification in future studies. In Figure S1a, the presence of two correlation phases, which have not been identified, overlapping with the phase PKP in distance range ~120°–160° explains the poor fit with the predicted time curve.

In the late coda window, the main contribution to the correlation wavefield comes from waves that reverberate nearly vertically (as shown in a recent study by Sens-Schönfelder et al., 2015) so that surface waves are largely suppressed. All phases identified in the correlation wavefield correspond to differences between seismic arrivals with the same ray parameter and a subset of propagation legs in common. Huygen's principle can be used to predict the timing of all arrivals using a virtual source positioned at major seismic boundaries in the Earth. This mechanism explains both features with the time behavior of regular seismic phases and those previously unexplained differential phases.

The correlation procedure provides a new view of the seismic wavefield and allows efficient extraction of seismic signals that might lie below the typical noise level in conventional seismology.

Acknowledgments
We thank B. Tauzin for helpful discussions. The synthetic experiment was performed on the ANU Terrawulf cluster, a computational facility developed with support from the AuScope initiative. AuScope Ltd. is funded under the National Collaborative Research Infrastructure Strategy (NCRIS), an Australian Commonwealth Government Programme. The facilities of IRIS Data Services, and specifically the IRIS Data Management Center, were used for access to waveforms, related metadata, and/or derived products used in this study. Waveform data used in this study are from IRIS/IDA Seismic Network (https://doi.org/10.7914/SN/II) operated by Scripps Institution of Oceanography (SIO), Global Seismograph Network (https://doi.org/10.7914/SN/IU) operated by Albuquerque Seismological Laboratory (ASL)/USGS and Australian National Seismograph Network operated by Geoscience Australia (GA). We thank P. Poli and an anonymous reviewer for their insightful reviews.

References

Bensen, G. D., Ritzwoller, M. H., Barmin, M. P., Levshin, A. L., Lin, F., Moschetti, M. P., et al. (2007). Processing seismic ambient noise data to obtain reliable broad-band surface wave dispersion measurements. *Geophysical Journal International*, *169*(3), 1239–1260. https://doi.org/10.1111/j.1365-246X.2007.03374.x

Boschi, L., & Weemstra, C. (2015). Stationary-phase integrals in the cross correlation of ambient noise. *Reviews of Geophysics*, *53*, 411–451. https://doi.org/10.1002/2014RG000455

Boué, P., Poli, P., Campillo, M., Pedersen, H., Briand, X., & Roux, P. (2013). Teleseismic correlations of ambient seismic noise for deep global imaging of the Earth. *Geophysical Journal International*, *194*(2), 844–848. https://doi.org/10.1093/gji/ggt160

Boué, P., Poli, P., Campillo, M., & Roux, P. (2014). Reverberations, coda waves and ambient noise: Correlations at the global scale and retrieval of the deep phases. *Earth and Planetary Science Letters*, *391*, 137–145. https://doi.org/10.1016/j.epsl.2014.01.047

Buland, R., & Chapman, C. H. (1983). The computation of seismic travel times. *Bulletin of the Seismological Society of America*, *73*(5), 1271–1302.

Campillo, M., & Paul, A. (2003). Long-range correlations in the diffuse seismic coda. *Science*, *299*(5606), 547–549. https://doi.org/10.1126/science.1078551

Crotwell, H. P., Owens, T. J., & Ritsema, J. (1999). The TauP toolkit: Flexible seismic travel-time and ray-path utilities. *Seismological Research Letters*, *70*(2), 154–160. https://doi.org/10.1785/gssrl.70.2.154

Ekström, G., Nettles, M., & Dziewoński, A. M. (2012). The global CMT project 2004–2010: Centroid-moment tensors for 13,017 earthquakes. *Physics of the Earth and Planetary Interiors*, *200-201*, 1–9. https://doi.org/10.1016/j.pepi.2012.04.002

Huang, H.-H., Lin, F.-C., Tsai, V. C., & Koper, K. D. (2015). High-resolution probing of inner core structure with seismic interferometry. *Geophysical Research Letters*, *42*, 10,622–10,630. https://doi.org/10.1002/2015GL066390

Kennett, B. L. N., Engdahl, E. R., & Buland, R. (1995). Constraints on seismic velocities in the Earth from traveltimes. *Geophysical Journal International*, *122*(1), 108–124. https://doi.org/10.1111/j.1365-246X.1995.tb03540.x

Lin, F.-C., Ritzwoller, M. H., Townend, J., Bannister, S., & Savage, M. K. (2007). Ambient noise Rayleigh wave tomography of New Zealand. *Geophysical Journal International*, *170*(2), 649–666. https://doi.org/10.1111/j.1365-246X.2007.03414.x

Lin, F.-C., & Tsai, V. C. (2013). Seismic interferometry with antipodal station pairs. *Geophysical Research Letters*, *40*, 4609–4613. https://doi.org/10.1002/grl.50907

Lin, F.-C., Tsai, V. C., Schmandt, B., Duputel, Z., & Zhan, Z. (2013). Extracting seismic core phases with array interferometry. *Geophysical Research Letters*, *40*(6), 1049–1053. https://doi.org/10.1002/grl.50237

Montagner, J.-P., & Kennett, B. L. N. (1996). How to reconcile body-wave and normal-mode reference Earth models. *Geophysical Journal International*, *125*(1), 229–248. https://doi.org/10.1111/j.1365-246X.1996.tb06548.x

Nishida, K. (2013). Global propagation of body waves revealed by cross-correlation analysis of seismic hum. *Geophysical Research Letters*, *40*, 1691–1696. https://doi.org/10.1002/grl.50269

Nissen-Meyer, T., van Driel, M., Stähler, S. C., Hosseini, K., Hempel, S., Auer, L., et al. (2014). AxiSEM: Broadband 3-D seismic wavefields in axisymmetric media. *Solid Earth*, *5*(1), 425–445. https://doi.org/10.5194/se-5-425-2014

Phạm, T.-S., & Tkalčić, H. (2017). On the feasibility and use of teleseismic *P* wave coda autocorrelation for mapping shallow seismic discontinuities. *Journal of Geophysical Research: Solid Earth*, *122*, 3776–3791. https://doi.org/10.1002/2017JB013975

Poli, P., Campillo, M., & de Hoop, M. (2017). Analysis of intermediate period correlations of coda from deep earthquakes. *Earth and Planetary Science Letters*, *477*, 147–155. https://doi.org/10.1016/j.epsl.2017.08.026

Poli, P., Pedersen, H. A., Campillo, M., & the POLENET/LAPNET Working Group (2012). Emergence of body waves from cross-correlation of short period seismic noise. *Geophysical Journal International*, *188*(2), 549–558. https://doi.org/10.1111/j.1365-246X.2011.05271.x

Ruigrok, E., Draganov, D., & Wapenaar, K. (2008). Global-scale seismic interferometry: Theory and numerical examples. *Geophysical Prospecting*, *56*(3), 395–417. https://doi.org/10.1111/j.1365-2478.2008.00697.x

Sens-Schönfelder, C., Snieder, R., & Stähler, S. C. (2015). The lack of equipartitioning in global body wave coda. *Geophysical Research Letters*, *42*, 7483–7489. https://doi.org/10.1002/2015GL065108

Shapiro, N. M., & Campillo, M. (2004). Emergence of broadband Rayleigh waves from correlations of the ambient seismic noise. *Geophysical Research Letters*, *31*, L07614. https://doi.org/10.1029/2004GL019491

Shapiro, N. M., Campillo, M., Stehly, L., & Ritzwoller, M. H. (2005). High-resolution surface-wave tomography from ambient seismic noise. *Science*, *307*(5715), 1615–1618. https://doi.org/10.1126/science.1108339

Snieder, R. (2004). Extracting the Green's function from the correlation of coda waves: A derivation based on stationary phase. *Physical Review E*, *69*(4), 046610. https://doi.org/10.1103/PhysRevE.69.046610

Stein, S., & Wysession, M. (2003). *An introduction to seismology, earthquakes, and earth structure*. (Chap. 3). Malden, MA: Blackwell Publishing.

Tkalčić, H. (2017). *The Earth's inner core revealed by observational seismology*. Cambridge, UK: Cambridge University Press. https://doi.org/10.1017/9781139583954

Wang, T., Song, X., & Xia, H. H. (2015). Equatorial anisotropy in the inner part of Earth's inner core from autocorrelation of earthquake coda. *Nature Geoscience*, *8*(3), 224–227. https://doi.org/10.1038/ngeo2354

Wapenaar, K., Draganov, D., Snieder, R., Campman, X., & Verdel, A. (2010). Tutorial on seismic interferometry: Part 1—Basic principles and applications. *Geophysics*, *75*(5), 75A195–75A209. https://doi.org/10.1190/1.3457445

Xia, H. H., Song, X., & Wang, T. (2016). Extraction of triplicated PKP phases from noise correlations. *Geophysical Journal International*, *205*(1), 499–508. https://doi.org/10.1093/gji/ggw015

Zhan, Z., Ni, S., Helmberger, D. V., & Clayton, R. W. (2010). Retrieval of Moho-reflected shear wave arrivals from ambient seismic noise. *Geophysical Journal International*, *182*(1), 408–420. https://doi.org/10.1111/j.1365-246X.2010.04625.x